

A quantum equation of motion for chemical reaction systems on an adiabatic double-well potential surface in solution based on the framework of mixed quantum-classical molecular dynamics

Atsushi Yamada and Susumu Okazaki

Citation: *The Journal of Chemical Physics* **128**, 044507 (2008); doi: 10.1063/1.2825611

View online: <http://dx.doi.org/10.1063/1.2825611>

View Table of Contents: <http://scitation.aip.org/content/aip/journal/jcp/128/4?ver=pdfcov>

Published by the [AIP Publishing](#)

Articles you may be interested in

[A molecular dynamics study of intramolecular proton transfer reaction of malonaldehyde in solutions based upon mixed quantum-classical approximation. I. Proton transfer reaction in water](#)

J. Chem. Phys. **141**, 084509 (2014); 10.1063/1.4893933

[2D IR spectra of cyanide in water investigated by molecular dynamics simulations](#)

J. Chem. Phys. **139**, 054506 (2013); 10.1063/1.4815969

[The roles of electronic exchange and correlation in charge-transfer-to-solvent dynamics: Many-electron nonadiabatic mixed quantum/classical simulations of photoexcited sodium anions in the condensed phase](#)

J. Chem. Phys. **129**, 164505 (2008); 10.1063/1.2996350

[The structures of ozone and H O x radicals in aqueous solution from combined quantum/classical molecular dynamics simulations](#)

J. Chem. Phys. **124**, 194502 (2006); 10.1063/1.2198818

[Dissipative mixed quantum-classical simulation of the aqueous solvated electron system](#)

J. Chem. Phys. **116**, 8418 (2002); 10.1063/1.1468886



A quantum equation of motion for chemical reaction systems on an adiabatic double-well potential surface in solution based on the framework of mixed quantum-classical molecular dynamics

Atsushi Yamada and Susumu Okazaki^{a)}

Institute for Molecular Science, Myodaiji, Okazaki 444-8585, Japan

(Received 24 August 2007; accepted 27 November 2007; published online 29 January 2008)

We present a quantum equation of motion for chemical reaction systems on an adiabatic double-well potential surface in solution in the framework of mixed quantum-classical molecular dynamics, where the reactant and product states are explicitly defined by dividing the double-well potential into the reactant and product wells. The equation can describe quantum reaction processes such as tunneling and thermal excitation and relaxation assisted by the solvent. Fluctuations of the zero-point energy level, the height of the barrier, and the curvature of the well are all included in the equation. Here, the equation was combined with the surface hopping technique in order to describe the motion of the classical solvent. Applying the present method to model systems, we show two numerical examples in order to demonstrate the potential power of the present method. The first example is a proton transfer by tunneling where the high-energy product state was stabilized very rapidly by solvation. The second example shows a thermal activation mechanism, i.e., the initial vibrational excitation in the reactant well followed by the reacting transition above the barrier and the final vibrational relaxation in the product well. © 2008 American Institute of Physics. [DOI: 10.1063/1.2825611]

I. INTRODUCTION

The chemical reaction in solution is, in general, described by a transition of a solute from the reactant state to the product state in a double-well potential energy surface. Then, quantum effects of the nuclei involved in the reaction play a very important role in various reaction processes. For example, tunneling is the purely quantum effect, which is noticeable for the light atoms such as proton. Molecular vibration also shows significant quantum effect in the thermal activation process surmounting the potential barrier since the energy gap between the vibrational states is much greater than the thermal energy even for the ordinary molecules. For example, it is about 3600 cm^{-1} for OH stretching, which is about 35 times greater than the thermal energy at room temperature, $\frac{1}{2}kT \sim 104\text{ cm}^{-1}$. The zero-point energy, $\sim 1800\text{ cm}^{-1}$, is great, too. It pushes up the system energy from a bottom of the well, contributing to the reaction rate.

In solution, solvent molecules provide the transition energy to the solute or absorb it from the solute promoting the vibrational excitation and relaxation, respectively. It accelerates the tunneling and reaction transition, too, by compensating the difference of the energy level between the reactant and product states keeping the energy conservation low.

In order to describe the quantum dynamics of chemical reaction systems in solution according to the earlier picture, it is essential to define the reactant and product state separately. Between the two states, first, the stable position of the proton is different and, further, the electronic states of the

donor and acceptor or the partial charges on them are considerably different from each other. Then, the solvent molecules around them clearly distinguish these two states by their interaction. Now, it is natural to define the reactant and product states separately and consider that continuous interaction with the moving solvent causes the decoherence between them. In solution, the system may not be described permanently by a superposition of the reactant and product states. The situation in solution is very different from that found in vacuum.

However, considering the present computational power, it is impossible to simulate the chemical reaction dynamics in solution fully quantum mechanically. Then, an approximation is needed. In order to solve this problem, the path integral influence functional theory^{1,2} and mixed quantum-classical approximation³⁻²⁷ have been applied so far. In particular, the latter mixed quantum-classical approximation is adequate for simulating realistic molecules, where one or a few degrees of freedom of interest are handled quantum mechanically while the remaining solvent degrees of freedom are all described classically.

The mixed quantum-classical molecular dynamics simulation methods have been applied to the proton transfer reaction on the adiabatic double-well potential surface. At an early stage of the progress, calculations have been done fixing the proton to a particular state, i.e., the vibrational ground state in an adiabatic double-well potential^{3,4} or the one in a reactant or product state defined according to a diabaticlike picture.^{5,6} The calculated trajectory was analyzed to obtain a rate constant based upon the reactive flux formula.

After then, the method has been developed to describe

^{a)}Author to whom correspondence should be addressed. Electronic mail: okazaki@ims.ac.jp.

the transitions among the vibrational states of the proton,^{7–26} where the coupled equations of motion have been solved to obtain a trajectory of the both solute and solvent degrees of freedom. Two conventional methods have been adopted. The first one is based on the mean-field approximation^{7–11} and the other the adiabatic surface hopping method.^{12–26} In the first method, the proton spread over the two wells simultaneously and, at the same time, it spread over a number of adiabatic vibrational states. On the other hand, the latter adiabatic surface hopping method assumed fast decoherence among the adiabatic vibrational states. However, the method described just vibrational excitation and relaxation on the whole adiabatic double-well potential energy surface. The system still spread over the two wells without discriminating between the reactant and product states. Thus, these two calculations did not take account of the decoherence between the reactant and product states or give a picture of the chemical reaction. In other words, the system was always found in a “coherent” state between the reactant and product states, where no reaction proceeded.

In our previous paper,¹² a quantum mechanical equation of motion has been presented, in the framework of the mixed quantum-classical approximation, for the nuclei involved in the chemical reaction in solution, explicitly defining the reactant and product states following the diabatic representation. The solvent was assumed to follow the classical equation of motion, the motion of which presents a time-dependent potential for the quantum system causing transitions among the states. The equation can describe the chemical reaction itself, i.e., the transition from the reactant state to the product state, as well as the vibrational excitation and relaxation within each of the reactant and product potential surfaces. The tunneling was also included in the reaction dynamics described by this equation. The method may be applied to the system where the electronically excited states are important in the reaction.

The surface hopping technique was adopted in our previous numerical calculations¹² for a few model proton transfer reaction systems since force on the classical system is significantly dependent upon whether the quantum state is in the reactant state or in the product state. This implies that, seeing from the classical system, the fast decoherence limit was assumed. The calculations reproduced both thermal activation process and tunneling one as a reaction mechanism.

However, diabatic representation makes no sense when electronically excited state does not take part in the chemical reaction of interest, i.e., when the energy level of the electronically excited states is very high. In this case, the reaction proceeds just on an adiabatic double well potential, i.e., the electronic ground state.

In the present study, a quantum mechanical equation of motion is presented for the reacting nuclei on an adiabatic ground-state potential surface defining the reactant and product states explicitly. The equation can describe thermal activation process, i.e., vibrational excitation in the reactant state followed by a reacting transition from the vibrational excited state in the reactant state to a vibrational excited state in the product state and the final vibrational relaxation to the vibrational ground state in the product state. It can also represent

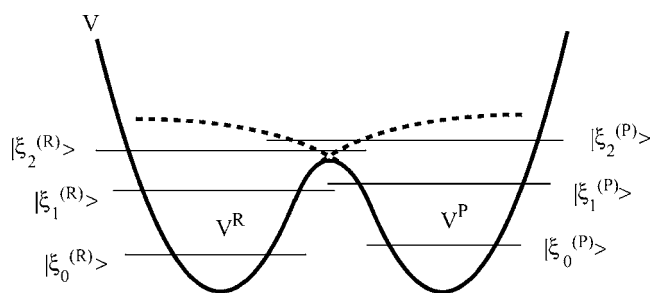


FIG. 1. Schematic pictures for the adiabatic potential energy surface V (thick solid line), the reactant potential energy surface V^R , and the product one V^P (thick dotted lines). The vibrational states in the reactant well, $\{|\xi_k^{(R)}\rangle\}$, and those in the product well, $\{|\xi_k^{(P)}\rangle\}$ (thin solid lines) are also presented.

the direct proton tunneling between the vibrational states of the reactant and product states lower than the potential barrier of the double well. In this case, however, the equation is more complicated than that obtained previously for the case of the diabatic representation,¹² although it is still calculable. Further, it includes a few approximations which must be tested before use.

Thus, together with our previous simulation method¹² in the diabatic representation, the present method in the adiabatic representation must present a set of powerful tools to simulate the chemical reaction in solution such as proton transfer reaction.

In Sec. II, we derive a quantum equation of motion for the nuclei involved in the chemical reaction defining the reactant and product states explicitly and, then, it is combined with the surface hopping method. In Sec. III, two numerical examples are presented in order to demonstrate the applicability of the present method, reproducing tunneling process and thermal activation process in model chemical reaction systems. The method is discussed in more detail in Sec. IV.

II. THEORY

First, we define a reactant potential energy surface and a product one by dividing an adiabatic ground state double-well potential surface into two surfaces. Then, we can write down a quantum mechanical equation of motion for the system of interest on the potential surfaces above. The system is coupled with the classical motion of the solvent according to the mixed quantum-classical molecular dynamics. Later, we combine our equation of motion with the surface hopping technique as an example.

A. Definition of the reactant and product states

We divide a double-well potential energy surface into the reactant and product potential energy surfaces and define the vibrational states in each potential energy surface as shown in Fig. 1. The two curves are drawn as follows. Below the potential barrier in the center, each curve is fitted to each of the two wells as correct as possible. The left and right walls are also well fitted for the reactant and product surfaces, respectively. However, slight arbitrariness may enter near the top of the barrier for the both surfaces. Above the barrier, the

lines (dotted lines) may be drawn almost arbitrarily. One primitive choice is to adapt two harmonic oscillators and another is to assume two Morse oscillators.

The points, here, are (1) each oscillator must reproduce the low-energy vibration in each of the two potentials below the barrier, (2) the wave functions of the excited vibrational states in the reactant and product surfaces must overlap sufficiently with each other at high energy levels above the barrier, and (3) we do not care much about the degree of the reproduction for the vibration above the barrier. Now, the vibrational states may be defined by the vibrational eigenstates in each of the reactant and product potential energy surfaces. These give a clear picture for the chemical reaction in the low energy region below the potential barrier. On the other hand, in the high energy region above the potential barrier, the system goes back and forth between the reactant and product states since the overlap of the wave functions between them is great. This corresponds to crossing and recrossing motions of the system above the barrier. If the frequency is much higher than that of the vibrational excitation and relaxation, then, the choice of the final state by the system may be considered to be a stochastic process where the solvent absorbs the vibrational excess energy of the solute. This may give a good model for the actual relaxation process. The great overlap of the vibrational wave functions between the reactant and product states above the potential barrier is essential for the inclusion of this kind of the stochastic relaxation to the final state. Of course, we have arbitrariness in the choice of the functional shape above the barrier. However, it is clear that the rate-determining step of the thermal activation process is not a reaction transition after the state is vibrationally excited above the barrier but the vibrational excitation itself. Thus, one candidate of the model surface is Morse function by which the potential may be well described below the barrier and, at the same time, the overlap of the wave functions between the reactant and product states above the barrier is great (see Fig. 1).

B. Quantum equation of motion

According to the mixed quantum-classical approximation, we start with the total Hamiltonian for the reacting solute degrees of freedom \mathbf{q} to be quantized of the form

$$\hat{H} = \hat{T} + \hat{V}_0(\mathbf{q}) + \hat{V}_I(\mathbf{q}; \mathbf{R}(t)) = \hat{T} + \hat{V}(\mathbf{q}; \mathbf{R}(t)), \quad (1)$$

where \hat{T} is the kinetic energy, \hat{V}_0 is the adiabatic double-well potential energy surface relevant to the chemical reaction in vacuum, and \hat{V}_I is the interaction with the solvent. Since $\mathbf{R}(t)$ represents trajectory of a set of solvent degrees of freedom including the solute ones to be handled classically, it works as a time-dependent parameter in the interaction potential, giving a time-dependent total potential \hat{V} for \mathbf{q} .

Now, in order to define the reactant and product states, $\hat{V}(\mathbf{q}; \mathbf{R}(t))$ is divided into two surfaces $\hat{V}^R(\mathbf{q}; \mathbf{R}(t))$ and $\hat{V}^P(\mathbf{q}; \mathbf{R}(t))$, respectively, according to the recipe presented in Sec. II A. Then, the vibrational states in the reactant potential

surface, $\{|\xi_k^{(R)}\rangle\}$, and those in the product one, $\{|\xi_k^{(P)}\rangle\}$, may be presented by solving the stationary-state Schrödinger equation

$$[\hat{T} + \hat{V}^R(\mathbf{q}; \mathbf{R}(t))]|\xi_k^{(R)}(\mathbf{q}; \mathbf{R}(t))\rangle = \varepsilon_k^{(R)}(\mathbf{R}(t))|\xi_k^{(R)}(\mathbf{q}; \mathbf{R}(t))\rangle, \quad (2)$$

$$[\hat{T} + \hat{V}^P(\mathbf{q}; \mathbf{R}(t))]|\xi_k^{(P)}(\mathbf{q}; \mathbf{R}(t))\rangle = \varepsilon_k^{(P)}(\mathbf{R}(t))|\xi_k^{(P)}(\mathbf{q}; \mathbf{R}(t))\rangle, \quad (3)$$

where $\varepsilon_k^{(R)}$ and $\varepsilon_k^{(P)}$ are the k th eigenvibrational energies within the reactant and product wells, respectively. Then, a wave function $|\Psi(t, \mathbf{q}; \mathbf{R}(t))\rangle$ may be expanded as

$$|\Psi(t, \mathbf{q}; \mathbf{R}(t))\rangle = \sum_k C_k^{(R)}(t)|\xi_k^{(R)}(\mathbf{q}; \mathbf{R}(t))\rangle + \sum_k C_k^{(P)}(t)|\xi_k^{(P)}(\mathbf{q}; \mathbf{R}(t))\rangle, \quad (4)$$

where $C_k^{(R)}(t)$ and $C_k^{(P)}(t)$ are the expansion coefficients for the k th vibrational state within the reactant well and the product one, respectively. Here, we must note that although each set of the vibrational states is orthonormalized, the two sets are not orthogonal each other. This will be discussed in detail later.

Substituting Eqs. (1) and (4) into the time-dependent Schrödinger equation, multiplying the vibrational state, $\langle \xi_l^{(R)} |$, from the left, and integrating over \mathbf{q} , we obtain

$$\begin{aligned} i\hbar(\dot{C}_l^{(R)} + \sum_k \dot{C}_l^{(P)} \langle \xi_l^{(R)} | \xi_k^{(P)} \rangle) \\ = \sum_k [\langle \xi_l^{(R)} | \hat{H} | \xi_k^{(R)} \rangle - i\hbar \langle \xi_l^{(R)} | \dot{\xi}_k^{(R)} \rangle] C_k^{(R)} \\ + \sum_k [\langle \xi_l^{(R)} | \hat{H} | \xi_k^{(P)} \rangle - i\hbar \langle \xi_l^{(R)} | \dot{\xi}_k^{(P)} \rangle] C_k^{(P)}. \end{aligned} \quad (5)$$

This is the equation of motion for the quantum system of interest. Solving this equation coupled with the classical equation of motion for the solvent, we can trace the time evolution of the quantum system in solution.

As a practical matter, it may be helpful to note here that Eq. (5) is of the form

$$i\hbar \mathbf{S} \dot{\mathbf{C}} = [\mathbf{H} - i\hbar \mathbf{D}] \mathbf{C}. \quad (6)$$

Here, the vector $\mathbf{C} = \{C_k^{(A)}\}$ and the matrices $\mathbf{S} = \{\langle \xi_l^{(A)} | \xi_k^{(B)} \rangle\}$, $\mathbf{H} = \{\langle \xi_l^{(A)} | \hat{H} | \xi_k^{(B)} \rangle\}$, and $\mathbf{D} = \{\langle \xi_l^{(A)} | \dot{\xi}_k^{(B)} \rangle\}$, where each A and B represents R or P . Since the form is not suitable for solving the differential equation numerically, we must calculate the inverse matrix of \mathbf{S} . Then, we obtain

$$i\hbar \dot{\mathbf{C}} = \mathbf{S}^{-1} [\mathbf{H} - i\hbar \mathbf{D}] \mathbf{C}. \quad (7)$$

Now, we can make usage of the ordinary numerical methods such as predictor-corrector method to solve this equation of motion.

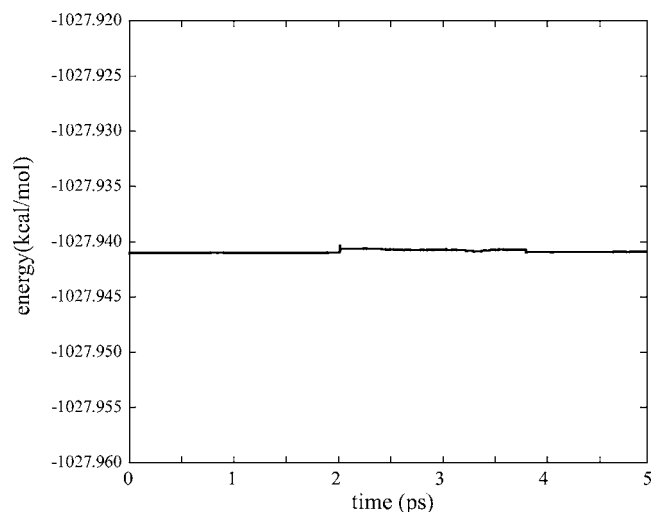


FIG. 2. Time evolution of the total energy ε of the total system.

C. The present basis functions and equation of motion

Further, we must discuss about the double completeness of the vibrational states $\{|\xi_k^{(R)}\rangle\}$ and $\{|\xi_k^{(P)}\rangle\}$ for the present reacting system. In principle, when the infinite expansion is done for the both wells, the description of the state will fail. Then, the equation of motion, Eq. (5) or (7), is of no sense. However, as discussed in Sec. II A, the vibrationally excited state we must take account of is the one which is found just above the barrier. Vibrationally excited states whose energy level is much higher than the barrier contribute little to the reaction dynamics. Thus, expansion may be cutoff at a proper state such that the probability that the system is found in the much higher states than the barrier is negligible. Then, the failure of the completeness of the eigenfunctions may be small.

In order to confirm the validity of the present quantum equation of motion, conservation of the total energy $\varepsilon = \langle \Psi | H | \Psi \rangle + \varepsilon_c$ of the total system was first examined along the trajectory obtained according to Eq. (5) or (7) together with the classical equation of motion. Here, ε_c is the total energy of the classical degrees of freedom which evolves by the Hellmann–Feynman force. The system examined here is the same as that presented later as example 1 in Sec. III B. The calculation was done in NVE ensemble for the isolated system without periodic boundary condition starting from a superposition of the states, Eq. (4), the diagonal terms of its density matrix giving the Boltzmann distribution. The result is presented in Fig. 2. Figure 2 clearly shows that the energy deviation is as small as 0.00003% of the total energy. Thus, the total energy is satisfactorily conserved.

D. Comparison with the equation of motion in the diabatic representation

We compare the present quantum equation of motion in the adiabatic representation with that in the diabatic representation.¹²

In the previous paper, we have presented an equation of

motion for the quantum system on the diabatic potential surface coupled with the classical degrees of freedom,

$$i\hbar \dot{C}_{ml}^{(d)} = \varepsilon_{ml}^{(d)} C_{ml}^{(d)} + \sum_{n(\neq m)} \sum_k \langle \xi_{ml}^{(d)} | V_{mn}^{(d)} | \xi_{nk}^{(d)} \rangle C_{nk}^{(d)} - i\hbar \sum_k \langle \xi_{ml}^{(d)} | \dot{\xi}_{mk}^{(d)} \rangle C_{mk}^{(d)}, \quad (8)$$

where $C_{ml}^{(d)}$ denotes the expansion coefficient of the wave function for the l th vibrational state in the m th diabatic electronic state, $\varepsilon_{ml}^{(d)}$ and $\xi_{ml}^{(d)}$ are the l th eigenvibrational energy and eigenvibrational function in the m th diabatic electronic state, respectively, and $V_{mn}^{(d)}$ is the electronic coupling element between the diabatic states m and n . The first term on the right-hand side of Eq. (8) works just for the phase. The second term gives the electronic transition from the (m, l) state to the (n, k) state, that is, the chemical reaction from the reactant state to the product state, which is caused by the electronic coupling $V_{mn}^{(d)}$ as well as the overlap between the vibrational states $\xi_{ml}^{(d)}$ and $\xi_{nk}^{(d)}$. The third term gives rise to the transition from the (m, l) state to the (m, k) state, corresponding to the vibrational excitation and relaxation within the m th diabatic potential. The equation of motion works well for the reaction system where an electronically excited state takes part in the reaction. In this case, the electronically ground and excited states are mixed in each vibrational state.

On the contrary, the equation of motion obtained in the present study plays an indispensable role when the electronic excited state is far from the ground state. Although arbitrariness is included in the definition of the vibrationally excited states above the barrier, the reactant and product states below the barrier are well defined. Comparing the shape of these two equations of motion, the chemical and physical meaning of each term of Eq. (8) for the diabatic representation is clearer than the slightly complicated one for the adiabatic representation in Eqs. (5) and (6).

E. Application of the surface hopping approximation

In this subsection, we show the mixed quantum-classical molecular dynamics method combining Eq. (7) with the framework of the surface hopping approach^{13,14} as an example of the numerical calculation method. The fewest switches algorithm^{13,14} is adopted here, too, in the same way as our previous study by the diabatic representation.

In the fewest switches algorithm, the time-dependent Schrödinger equation is solved to obtain the transition probability from the specified current state to the other states, then, the switching from the current state to the other state is determined by comparing a random number with the transition probability at every step time. In the present study, in order to conserve the total energy before and after the switching of the state, the velocity scaling is additionally performed for the classical particles.

Detail of the numerical method is almost the same as that of the previous study except for the followings. Due to the slightly complicated form of the Eq. (7), we adopted the coupling vector with the classical particle j to be the

force on it from the current quantum state, $-\langle \xi_k^{(P \text{ or } R)} | \partial H / \partial \mathbf{R}_j | \xi_k^{(P \text{ or } R)} \rangle$, giving a simple velocity scaling. This is a choice among many possibilities coming from the arbitrariness of the force from the quantum system on its transition.

III. NUMERICAL EXAMPLE

In this section, we show two numerical examples in order to demonstrate the ability of the present method combined with the surface hopping approximation, the first one representing the tunneling followed by the stabilization of the system by solvation and the second one the thermal activation and the barrier height fluctuation by the solvent.

A. Calculation

A solute is a model molecule constrained linearly in one dimension composed of a donor atom D and an acceptor atom A treated classically mechanically as well as a reacting quantum mechanical atom Q located between the donor and acceptor. An empirical valence bond model²⁸ was adopted for the double-well adiabatic potential function, where the reactant and product potential surfaces in vacuum were assumed to be those of harmonic oscillators described by D - Q and Q - A distances, respectively. The coupling between the reactant and the product was approximated to be a constant. The position of Q was described by the grid points with the interval of 0.01 Å. The solute was immersed in 255 flexible SPC water molecules^{29,30} in a cubic cell of length 19.4 Å in the periodic boundary condition. The system was controlled at constant temperature at 300 K using Nose–Hoover chain.³¹ The equation of motion was integrated using the Gear method with a time step of 0.01 fs. The intermolecular interaction was described by Coulombic and Lennard–Jones potentials, which was cut off for the pair whose distance is longer than 9 Å.

The vibrational state functions in solution were given by the linear combination of Hermite polynomial functions which are the eigenvibrational functions for the reactant and product surfaces in vacuum. The wave function in Eq. (4) was expanded by the vibrational eigenfunctions up to the third excited state for both of the reactant and product states.

B. Example 1: Tunneling process

The first example shows a proton transfer reaction, i.e., $Q=1$ g/mol. Point charges of the donor, proton, and acceptor in the reactant state were assumed to be 0.2, 0.1, and -0.3 , respectively, which change to be -0.6 , 0.1, and 0.5, respectively, in the product state. Positions of D and A were both constrained by imposing a harmonic potential of 100 kcal/mol Å² along the x coordinate with their centers separated by 2.6 Å. During the calculation, their y and z coordinates were fixed to be constant. The force constants for the D - Q and A - Q bonds were assumed to be the same as each other, i.e., 400 kcal/mol Å² and these equilibrium bond lengths were both set to be 1.0 Å. Then, the energy gap

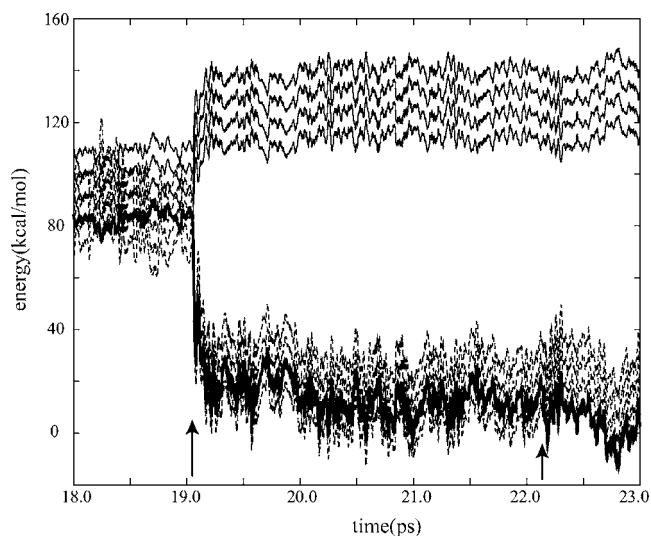


FIG. 3. Time evolution of the quantum system of example 1. Four thin solid lines represent the vibrational energy levels in the reactant well, four thin dotted lines the vibrational energy levels in the product well, and the thick solid line the current vibrational energy level specified by the surface hopping method.

between the eigenvibrational states in vacuum was 8.7 kcal/mol for each well. The coupling between the reactant and product was 10 kcal/mol.

Figures 3–5 show the result of the time evolution of the vibrational energy levels for the reactant state and the product state. Figures 4 and 5 are the expanded figures of Fig. 3 around $t=19.05$ and 22.14 ps (arrows in Fig. 3), respectively.

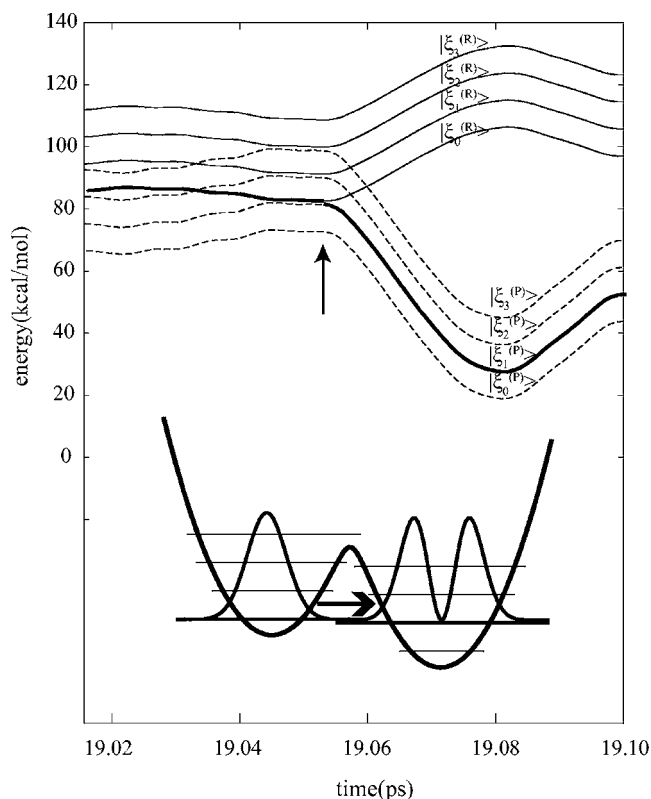


FIG. 4. Expanded figure of Fig. 3 when a tunneling transition occurred from the vibrational ground state in the reactant well, $|\xi_0^{(R)}\rangle$, to the vibrational excited state in the product well, $|\xi_1^{(P)}\rangle$.

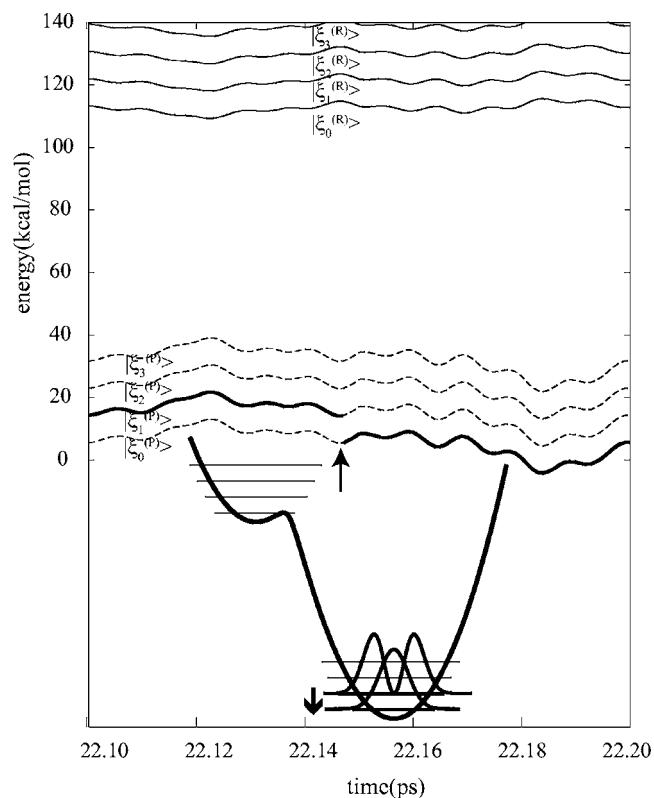


FIG. 5. Expanded figure of Fig. 3 when a vibrational relaxation occurred from the vibrational excited state in the product well, $|\xi_1^{(P)}\rangle$, to the vibrational ground state in the same well, $|\xi_0^{(P)}\rangle$.

The thick solid line represents the current vibrational state chosen by the surface hopping method. An initial state was set to be the vibrational ground state in the reactant well, $|\xi_0^{(R)}\rangle$. A reacting transition from the reactant vibrational ground state $|\xi_0^{(R)}\rangle$ to the vibrational first excited state in the product well, $|\xi_1^{(P)}\rangle$, occurred at $t=19.05$ ps as shown in Fig. 4. This is a tunneling transfer. The height of the potential barrier was, then, about 22.0 kcal/mol, which is higher than the two vibrational states above. The difference of energy 1.0 kcal/mol between the two states, $|\xi_0^{(R)}\rangle$ and $|\xi_1^{(P)}\rangle$, was supplied by the solvent. Then, after the reaction transition, stabilization of the product state occurred by the solute-solvent interaction, i.e., the solvation dynamics after the reorganization of the electronic state of the solute molecule. The unstable product state was, thus, stabilized by solvation by as much as 80 kcal/mol. Subsequent vibrational relaxation occurred at $t=22.14$ ps to the vibrational ground state in the product well, $|\xi_0^{(P)}\rangle$, as shown in Fig. 5 to complete the reaction.

C. Example 2: Thermal activation process

The second example is the thermal activation process where the system surmounts the potential barrier quantum mechanically. Here, the mass of the atom Q was assumed to be 10 g/mol. The point charges of D , Q , and A in the reactant well were assumed to be 0.0, 0.2, and -0.2 , respectively, which change to be -0.2 , 0.2, and 0.0 in the product well, respectively. Positions of D and A were both constrained by imposing a harmonic potential of 200 kcal/mol \AA^2 along x

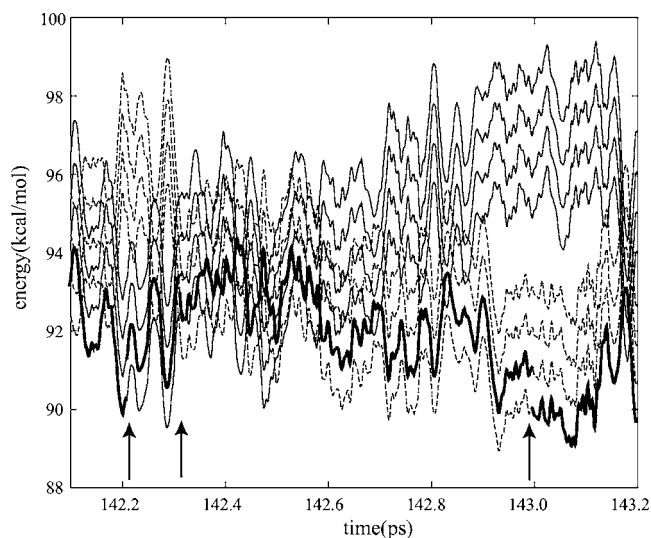


FIG. 6. Time evolution of the quantum system of example 2. Four thin solid lines represent the vibrational energy levels in the reactant well, four thin dotted lines the vibrational energy levels in the product well, and the thick solid line the current vibrational energy level specified by the surface hopping method.

coordinate with their centers separated by 2.9 \AA . During the calculation, their y and z coordinates were fixed to be constant. The force constants for the $D-Q$ and $A-Q$ bonds were set to be the same as 40 kcal/mol \AA^2 and these equilibrium bond lengths were both set to be 1.2 \AA . Then, the energy gap between vibrational states in vacuum was 0.88 kcal/mol for each well. Vibrational states in solution were described in the same way as example 1. The coupling between the reactant and product states was assumed to be 2.0 kcal/mol.

The results are shown in Figs. 6–8. All kinds of lines are the same as the case of the first example in Figs. 3–5. The transition from the vibrational ground state in the reactant well, $|\xi_0^{(R)}\rangle$, to the vibrational first excited state in the same well, $|\xi_1^{(R)}\rangle$, occurred at $t=142.21$ ps as shown in Figs. 6 and 7. After the vibrational excitation, the vibrational energy level became higher than the potential barrier. Then, the reacting transition from $|\xi_1^{(R)}\rangle$ to the vibrational first excited state in the product well, $|\xi_1^{(P)}\rangle$, occurred at $t=142.31$ ps, which was followed by the vibrational relaxation from $|\xi_1^{(P)}\rangle$ to the vibrational ground state in the product well, $|\xi_0^{(P)}\rangle$, at $t=143.00$ ps to complete the chemical reaction as shown in Figs. 6 and 8. The process gives an example of the thermal activation combined with the barrier level fluctuation.

IV. DISCUSSION

In the present paper, we have proposed a quantum equation of motion for a solute in solution on an adiabatic potential energy surface based on the framework of mixed quantum-classical molecular dynamics. It was combined with the surface hopping approach as an example. Then, we showed two numerical examples of the present method, tracing the model systems for chemical reaction dynamics in solution.

As shown in the second example, the vibrational excitation in the reactant well was an essential process in the first stage of the thermal activation mechanism. In the vibrational

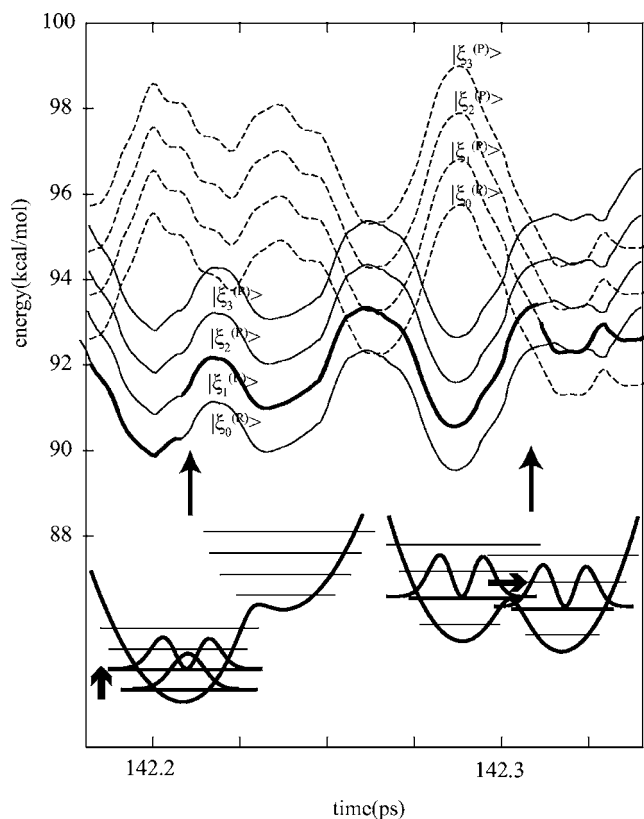


FIG. 7. Expanded figure of Fig. 6 when a vibrational excitation occurred from the vibrational ground state, $|\xi_0^{(R)}\rangle$, to the vibrational excited state, $|\xi_1^{(R)}\rangle$, in the reactant well, which was followed by reacting transition above the barrier from the vibrational excited state in the reactant well, $|\xi_1^{(R)}\rangle$, to the vibrational excited state in the product well, $|\xi_1^{(P)}\rangle$.

excited state, only one transition occurred from the reactant state to the product state before the system was stabilized finally in the product well. Based on the harmonic potential functions for the two wells in this example, the overlap between the vibrational excited states in the reactant and product wells may be underestimated. This may be improved when we adopt the Morse potential where the crossing and recrossing motions must be found frequently in the excited states. Since the rate determining step of the chemical reaction must be the vibrational excitation in the reactant well, ambiguity of the definition of the reactant and product potential energy surfaces above the potential barrier may not matter so much.

In addition to the proton transfer reaction, the method may be applied to the general double-well potential systems including isomerization reaction. Furthermore, this method can be easily extended to QM/MM type calculation to evaluate the accurate adiabatic potential surface in solution at every simulation step. Further, if a new approximation theory, which can describe the dynamics of the classical and quantum systems beyond the surface hopping approximation, is developed, the present equation of motion may easily be implemented in such new mixed quantum-classical method. Together with the previous equation of motion based upon the diabatic representation, the present method must work as one of the powerful tools to trace the molecular mechanism of the chemical reactions in solution.

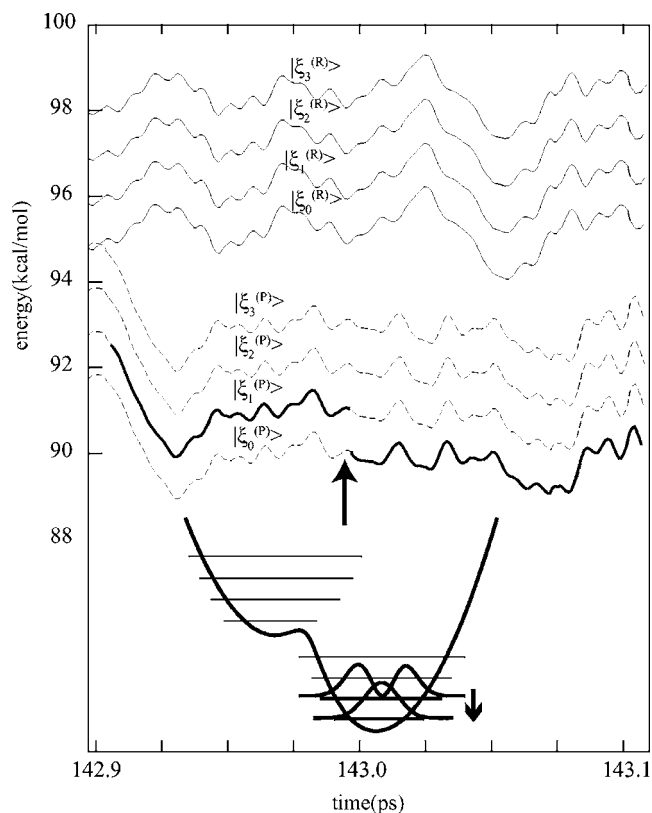


FIG. 8. Expanded figure of Fig. 6 when a vibrational relaxation occurred from the vibrational excited state in the product well, $|\xi_1^{(P)}\rangle$, to the vibrational ground state in the same well, $|\xi_0^{(P)}\rangle$.

V. CONCLUSION

A quantum equation of motion has been presented for the reacting nuclei on an adiabatic double-well potential surface coupled with the classical solvent degrees of freedom, where the reactant and product states are defined explicitly by dividing the double-well potential into reactant and product wells. The equation can describe well the quantum effects of the nuclei relevant to the reaction such as tunneling, zero-point energy, and thermal activation, that is, vibrational excitation followed by reacting transition and the final vibrational relaxation. In order to complete the framework of the mixed quantum-classical molecular dynamics method, the present quantum dynamics was combined with the surface hopping technique, as an example. Two numerical examples were also presented demonstrating the potential power of the present method, where the first one could trace the tunneling process followed by the stabilization of the system by the solvation dynamics and the second one showed the reaction by the thermal activation mechanism.

ACKNOWLEDGMENTS

The authors would like to thank Professor H. Nakamura at IMS and Professor A. Morita at Tohoku University for their kind discussions. This work was supported by the Next Generation Super Computing Project, Nano Science Program, MEXT, Japan and was also supported in part by Grant-in-Aid for Scientific Research (17105001 and 18066020) from Japan Society for the Promotion of Science (JSPS). The

calculations were carried out on the computers at Okazaki Research Center for Computational Science, National Institutes of Natural Sciences.

- ¹M. Grifoni and P. Hänggi, *Phys. Rep.* **304**, 229 (1998).
- ²M. Thorwart, M. Grifoni, and P. Hänggi, *Ann. Phys.* **293**, 15 (2001).
- ³D. Borgis, G. Tarjus, and H. Azzouz, *J. Chem. Phys.* **97**, 1390 (1992).
- ⁴D. Borgis, G. Tarjus, and H. Azzouz, *J. Phys. Chem.* **96**, 3188 (1992).
- ⁵H. Azzouz and D. Borgis, *J. Chem. Phys.* **98**, 7361 (1993).
- ⁶A. Staib, D. Borgis, and J. T. Hynes, *J. Chem. Phys.* **102**, 2487 (1995).
- ⁷S. R. Billeter and W. F. van Gunsteren, *Comput. Phys. Commun.* **107**, 61 (1997).
- ⁸S. R. Billeter and W. F. van Gunsteren, *J. Phys. Chem. A* **104**, 3276 (2000).
- ⁹P. Bala, B. Lesyng, and J. A. McCammon, *Chem. Phys.* **180**, 271 (1994).
- ¹⁰P. Bala, P. Grochowski, B. Lesyng, and J. A. McCammon, *J. Phys. Chem.* **100**, 2535 (1996).
- ¹¹P. Bala, P. Grochowski, K. Nowiński, B. Lesyng, and J. A. McCammon, *Biophys. J.* **79**, 1253 (2000).
- ¹²A. Yamada and S. Okazaki, *J. Chem. Phys.* **124**, 094110 (2006).
- ¹³J. C. Tully, *J. Chem. Phys.* **93**, 1061 (1990).
- ¹⁴S. Hammes-Schiffer and J. C. Tully, *J. Chem. Phys.* **101**, 4657 (1994).
- ¹⁵S. Hammes-Schiffer and J. C. Tully, *J. Phys. Chem.* **99**, 5793 (1995).
- ¹⁶J. C. Tully, *Faraday Discuss.* **110**, 407 (1998).
- ¹⁷D. Kohen, F. H. Stillinger, and J. C. Tully, *J. Chem. Phys.* **109**, 4713 (1998).
- ¹⁸J. Morelli and S. Hammes-Schiffer, *Chem. Phys. Lett.* **269**, 161 (1997).
- ¹⁹K. Drukker, S. W. de Leeuw, and S. Hammes-Schiffer, *J. Chem. Phys.* **108**, 6799 (1998).
- ²⁰J.-Y. Fang and S. Hammes-Schiffer, *J. Chem. Phys.* **110**, 11166 (1999).
- ²¹H. Decornez, K. Drukker, and S. Hammes-Schiffer, *J. Phys. Chem. A* **103**, 2891 (1999).
- ²²S. P. Webb and S. Hammes-Schiffer, *J. Chem. Phys.* **113**, 5214 (2000).
- ²³S. R. Billeter, S. P. Webb, T. Lordanov, P. K. Agarwal, and S. Hammes-Schiffer, *J. Chem. Phys.* **114**, 6925 (2001).
- ²⁴S. R. Billeter, S. P. Webb, P. K. Agarwal, T. Iordanov, and S. Hammes-Schiffer, *J. Am. Chem. Soc.* **123**, 11262 (2001).
- ²⁵P. K. Agarwal, S. R. Billeter, and S. Hammes-Schiffer, *J. Phys. Chem. B* **106**, 3283 (2002).
- ²⁶S. Y. Kim and S. Hammes-Schiffer, *J. Chem. Phys.* **119**, 4389 (2003).
- ²⁷T. Terashima, M. Shiga, and S. Okazaki, *J. Chem. Phys.* **114**, 5663 (2001).
- ²⁸U. W. Schmitt and G. A. Voth, *J. Phys. Chem. B* **102**, 5547 (1998).
- ²⁹O. Teleman, B. Jönsson, and S. Engström, *Mol. Phys.* **60**, 193 (1987).
- ³⁰A. Wallqvist and O. Teleman, *Mol. Phys.* **74**, 515 (1991).
- ³¹G. J. Martyna and M. L. Klein, *J. Chem. Phys.* **97**, 2635 (1992).